LAWRENCE
LIVERMORE
NATIONAL
LABORATORY

LLNL-CONF-656673

Laser Deflagration-to-Detonation in Keto-RDX doped with Resonant Hollow Gold Nanoshells

P. R. Wilkins

July 7, 2014

15th International Detonation Symposium
San Francisco, CA, United States
July 13, 2014 through July 18, 2014

Disclaimer

LLNL-CONF-656673

Laser Deflagration-to-Detonation in Keto-RDX doped with Resonant Hollow Gold Nano-shells

Paul. R. Wilkins*

*High Explosives Applications Facility Mailstop L-281
Lawrence Livermore National Laboratory[a], Livermore, CA 94550

Abstract. 2-Oxo-1,3,5-trinitro-1,3,5-triazacyclohexane (Keto-RDX or K-6), the most powerful energetic material among nitrourea secondary explosives, is utilized in an laser initiated Deflagration-to-Detonation (DDT) detonator that takes advantage of a short column length and milliJoule initiation thresholds without the drawbacks of a primary explosive such as CP and its attendant electrical and shock sensitivity. The combination of Mie resonant hollow gold nano-shells (HGNs) intermixed with the explosive allows for very rapid laser heating of the highly exothermic explosive in a package that is naturally lightning-safe. The dopant level of the HGNs is at 0.1% by weight or lower, typically below the background solvent contaminant for most explosives and this nanoscale material does not photosaturate at high intensities like dyes, which would otherwise limit the energy absorption. The doped K-6 is pressed into a brass body into a cavity 5 mm in diameter and 3 mm long at a density of ~75% bulk density with a fused silica window approximately 0.4 mm thick that is AR coated for 810 nm laser diode. Just over 10.8 watts of laser energy at a wavelength of 810 nm is relay imaged from a 100 μm core fiber with a lens to a spot size of ~800 μm upon the surface of the window. Measurements of the interior of the HE column shows that DDT transition occurred within 2 mm or less from the front optical window upon which the laser was focused. The dimensions of small gold nano-shells have an excitation wavelength of 810-nm tuned to the Mie resonance of the gold nano-shell. Ballistic electron transport allows the alternating electron density waves to drive free electrons back and forth from the poles at the optical frequency creating heating that does not photosaturate. This initiates an increase in temperature until the nano-shells melts back into a spherical droplet of gold. Thermocouple measurements of a mock material (PentaErythritol) doped at 0.05% show an increase to ~1800° C within milliseconds, with this heating rate measurement limited by the transient response of the small thermocouple. The highly exothermic decomposition of K-6 from 185°C to 195°C provides enough release of energy to transition from deflagration to detonation in 1-2 mm

[a] This work was performed under the auspices of the U.S. Department of Energy by Lawrence Livermore National Laboratory under contract DE-AC52-07NA27344. Lawrence Livermore National Security, LLC

from the focal point as the laser light is absorbed by the HGNs dispersed upon the surface of the K-6 particles.

The ball-milled K-6 was mixed with an aqueous solution of hollow gold nano-shells HGNs at a concentration of 10^{12} HGNs/cc and vigorously mixed to wet the particulates thoroughly with the water nano-shell solution and vacuum dried to the original weight of the K-6 material. As the nanoparticles dry upon the surface of the K-6 particles, with a dielectric index of air, the spectrophotometer curve shifts from the absorption in solution to a slightly longer wavelength in air where the dielectric index is lower than water as represented by spectrophotometer curve and that same solution dried as a film upon a flat microscope slide. This unique application of a DDT detonator using nano-resonant doped explosive with a secondary explosive that runs up to detonation in less than 3 mm, doing so at much lower doping levels than the traditional 1%-5% lampblack utilized in primary HE mixtures for other optical detonators. Full detonation was achieved with 130 milliJoules of energy using a free-space air transport laser beam focused to an 800 μm spot at a fluence of 2000 watts/cm^2 for 12.1 milliseconds upon HGN doped K-6. These 70 milligram K-6 samples fully reacted and swaged the brass body into the confinement cap showing high order detonation.

Low-Energy Laser Initiation of Explosives

The last two decades have seen development of laser-initiated detonators with the purpose of seeking higher margins of safety in detonators used in weapon systems and test-firing operations. Although high-power electrical detonators have an excellent safety record; current development work is focused towards reducing the possibility of accidental initiation by sources in nature (such as lightning) and has sought to provide an initiation source that has both electromagnetically immunity and has no natural counterpart. Towards this end, there has been significant development of new high-power detonators using a non-electrical source such as a short duration high-peak-power laser pulse. These laser detonators use low-efficiency pulsed lasers that usually employ Q-switching and pulse durations in the nanosecond regime. This paper examines a low-average power laser detonator using a highly-efficient thermal initiation mechanism to reduce the need for the high peak of q-switched lasers and their accompanying low electrical efficiency. These systems are low-average energy systems (tens of watts over milliseconds) of highly efficient diode lasers for low-energy optically initiated detonators, providing the advantage of an efficient diode laser source with low susceptibility from electrostatic or electromagnetic damage. Previous development work in this low-average-energy laser initiation regime used either primary explosives, which have their own intrinsic handling and packaging risks, or highly-doped materials for opto-thermal initiation using carbon-black or other adulterants added at a mass-ratio of 1% to 5% of the total explosive material.[2] This research investigates the novel idea of incorporating a very low mass-ratio (less than 0.1% by weight) dopant of HGNs onto the surface of suitable secondary explosive crystals that detonate when heated rapidly. Unique to this concept, these gold nano-shells have been designed to be resonantly absorptive at a specific wavelength band. These HGNs do not

photosaturate like ordinary dyes as long as they remain in their hollow geometry and will stop absorbing only upon melting and reconsolidation into another geometry (molten sphere). When an aqueous solution of these HGNs are mixed with explosives and the water allowed to evaporate, the HGNs coat the surface of the explosive crystals with dozens of HGNs per crystal. This allows for a distribution of tiny hot dipole resonators that are mixed in at a very high density (~10^{12} per gram of material) to act as distributed hot-spots within the pressed explosive load when illuminated by laser radiation. Within the explosive mixture, these tiny HGNs then act to replace the normally shock-induced hotspots from PdV work on gas compression by pore collapse of the voids in a pressed explosive from an initiating shockwave usually caused by impact or shock compression.

Absorption Curves of Hollow Gold Nano-shells

This resonant absorption of the HGNs is achieved by tuning the classic Mie resonance of a conducting sphere into a dipole resonance mode by careful tailoring of the surface plasmon wavelength at the gold-dielectric interface to be an integral value of the circumference. These nano-shells are on the order of 43 nm in diameter and the resonance follows the classic approximation for surface plasmon wavelength where the surface plasmon wavelength is far shorter than the excitation wavelength of light (810 nanometers) and the symbol ε_m and ε_d represent the dielectric function of the metal and dielectric respectively as show in equation 1.

$$\lambda_{SP}=\lambda\sqrt{\frac{(\varepsilon_m+\varepsilon_d)}{(\varepsilon_m\varepsilon_d)}} \qquad (1)$$

Figure 1 illustrates the tuned HGN absorption curve for a suspension of nano-shells in water as a function of wavelength for both a solution of nano-shells in water and a projected curve for an air-dried film. The absorption curve also shows the quadrapole resonance, which is less efficient at relative absorption, seen as the small side peak to the right of the peak absorption. The absorption curve shift that occurs when the solvent is removed by evaporation and the nano-shells are evaporated onto a surface is due to the change in surface plasmon wavelength at the gold-dielectric interface as the dielectric constant shifts from water to an air dielectric.

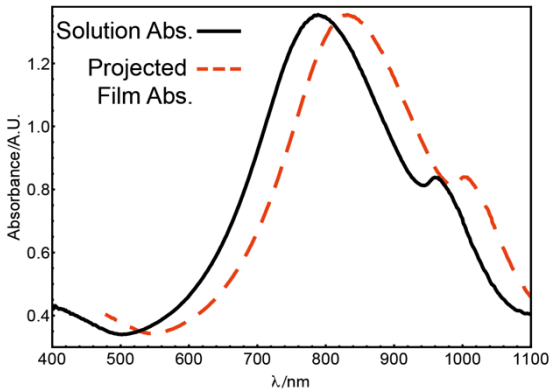

Figure 1. –Absorption curve of tuned HGNs

This is experimentally verified by evaporation of a drop of the HGN solution upon a glass slide after a batch of HGNs is made per reference (1) and centrifuged to increase concentration. Figure 2 shows an actual absorption measurement made of a diluted (~10^{-6}) aqueous sample of HGNs from a prepared batch and a thin film dried upon a microscope slide in the same spectrophotometer[2] and the resulting 40nm redshift of the absorption curve.

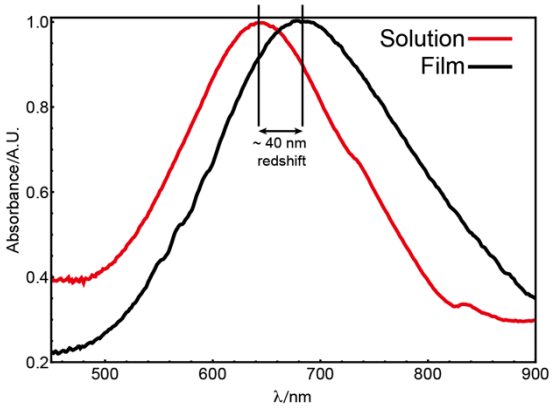

Figure 2. – Absorption offset for Dielectric Index

Mixing HE with Hollow Gold Nano-shells

[2] Perkin-Elmer LAMBDA 950 Spectrophotometer

Most conventional secondary explosives have no intrinsic absorption in the near IR band that is used to thermally heat these samples. To prepare the samples for enhanced absorption they were mixed with the HGNs aqueous solution and dried. Figure 3 shows that penetration depth for an aqueous solution as a function of nano-shell concentration and the iso-contour bands represent the percentage of light transmitted by penetration depth.

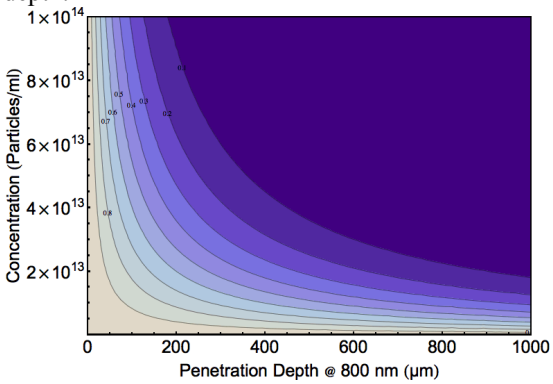

Figure 3 – Penetration depth vs. concentration

This graph is for a uniform refractive index and in contrast to that graph of solution, the pressed HE as a transparent powdered media is highly scattering and may not be well represented by this graph. In practice a deeper penetration is desired into the pressed HE to have the laser energy absorbed and heating a critical volume of HE hundreds of microns deep that can propagate as a building detonation. Almost all of these explosives that were tested (PETN, HMX, RDX, HNS, Keto-RDX [K-6], and Hexanitrohexaazaisowurtzitane are non-soluble in water and therefore will not dissolve if mixed with an aqueous HGNs suspension, therefore mixing them with the HGNs solution will not change the particle size distribution of the powder. The HGNs were prepared as outlined in Reference (1) and centrifuged. This HGNs suspension was mixed with equal amounts (1 ml for each gram) in unit batches of 2 grams of HE at a time. The HE was generally ball-milled to a specific relative surface area if not defined (such as with HNS IV) and as it is not wetted by water, must be agitated and forced into the aqueous solution until a smooth slurry is generated. Upon drying, the semi-caked dried HE slurry is gently rolled by a mortar against an aluminum evaporation pan until reduced to a fine loose powder similar in consistency to the ball-milled powder and the nanoshells add no appreciable mass to the HE samples.

Laser Detonators tests of Nano-shell doped HE

We tested powders at a variety of different densities starting with an initial gold nano-shell doped HE powder at a bulk density of 50% into a small brass detonator body. This brass cavity for holding the HE was 0.2 inches (5-mm) in diameter with a fused silica window 0.4mm thick (AR coated for 810-nm laser light for ~0.5% loss) at one end and a front surface mirror on the other end of the cavity to allow either light emission for breakout of the detonation or to impact a Dynasen piezo pin in the confinement cap, thus recording the explosive function time. Initial tests showed that a 50% bulk density was too low for a DDT detonator operation so a second mirror was added in a hand-press operation onto the first to compress the initial pressing to a density of approximately ~75% for a total column height of 3-mm. Figure 4 shows cross section of the laser detonator with the input fused silica window, the brass body, the HE load, and the output mirror as loaded.

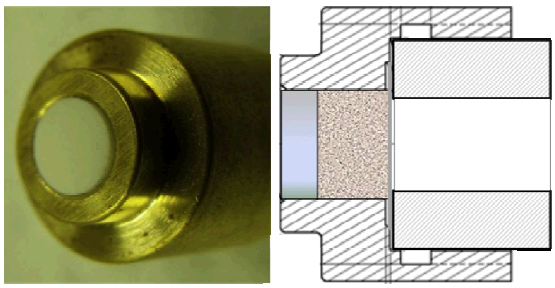

Figure 4. –Cross Section of Laser Det

The hand loading of the IP of these laser detonators was not well controlled and the next sequence of tests determined to use a steel die to press the pellets of nano-shell doped HE first and then load these pressed and weighed pellets into an integral brass body. The total mass loaded was approximately 65 to 70 milligrams per laser detonator based on the HE used. Of all HEs tested, the best performing explosive was Keto-

RDX (K-6) and HMX and poor showing by the rest. These other HEs did react, but did not transition to a detonation in the 3-mm column length, which was a desired minimal size. PETN performed the worst with frequent melting prior to any charring and no gas reaction, perhaps an attribute of the low melting point. A temperature heating test using an embedded 0.010" K-type thermocouple (Omega KMQXL-010U-12) embedded within a nano-shell doped mock HE fill of pentaerythritol at 0.5 mm from the fused silica window showed a temperature increase to ~1800^{o} C within 100 millieconds – the thermal response limited by the sampling rate of the meter. Clearly the temperature was high enough for deflagration although as a caveat this temperature is outside the normal operating range of a K-type thermocouple that is typically limited to a maximum of 1350^{o} C. The HMX usually (but not consistently) detonated in this configuration, and always reacted, but a column length of 3-mm may be too short to run to a full detonation and the results in terms of the firing times and integrated energies are shown in Table 1. Only K-6 consistently showed full detonation in all tests at a column length of 3 mm. This was using a total power of ~10 watts at a fluence of 2000 watts/cm^2 onto the fused silica window for 15 to 30 milliseconds. The reason for the success with K-6 may lay with its unique decomposition rate as it undergoes a 97% loss in weight from 185^{o} C-195^{o} C which indicates that the thermal decomposition of K-6 is highly exothermic in nature with almost single step decomposition reaction.[5] K-6 has the added advantage of being the most powerful of the nitrourea secondary explosives with an explosive output that is 104% that of HMX.[6] An oscilloscope recorded the timing of the laser light and recorded the breakout time of the Dynasen piezo pin. K-6 laser detonator firing times and integrated energies are shown Tables 2 and 3 for a focal spot of 1000 μm and 800 μm in diameter respectively. Minimum spot size achieve with this relayed fiber-coupled system was 800 μm.

Laser Illumination System for Detonation Tests

The laser used for these tests was an Apollo Laser Diode of 20 watts at 808.2 nanometer wavelength (F40-810-1P) driven by a low inductance driver (Apollo Laser D-5100PP Laser Driver) capable of switching on the 40-Amp drive power for the diode in less than 200 nanoseconds. A monitor photodiode provided timing of the laser light and for the initial tests of pulse duration as controlled by a Stanford delay generator that provides a 30-millisecond gated laser pulse. As this is a fiber coupled laser diode, the output beam from the 100 micron core fused silica fiber (NA 0.22) was collimated with a 50-mm focal length fused silica lens (AR coated) and transited a safety shutter onto a focusing lens of 50-mm focal length fused silica lens (AR Coated) that passed the beam through the uncoated Lexan debris shield over a port in the laser Detonator firing chamber. These Lexan plates were re-positioned following every shot as the debris from the fused silica window was embedded from the blast into the surface of the Lexan debris shield. Due to losses from the fiber coupling and lenses and transmission through a Lexan debris shield the power reaching the laser detonator mount inside the firing chamber was measured with a Coherent Laser Power Meter as a final transmitted power of 10.8 watts at 808.2 nm. Figure 6 at the end of this paper shows the optical test bench and it must be emphasized that the optical delivery system was a free-space air transport beam designed to test a wide range of explosives and fills without sacrificing expensive fibers and internal ball lenses as would be found in an optimized laser delivery system for a laser detonator. This optical test bench was created to simply use a common platform for laser light focused to an 800-micron spot size (1/e^2) at a power density of approximately 2000 watts/cm^2 at the center of the fused silica window for testing a variety of doped explosives with identical laser beam and fluence characteristics.

Results

The first results of laser initiation of HGN doped explosives show the viability of a secondary explosive detonator driven by a low-power laser source. The advantage of low-power laser initiation is the use of a safe secondary explosive, the relatively high electrical efficiency of the laser diode and small size and the low electrical power requirements for the applications that this device is

targeted towards. Non-optimized laser energies of 130-millijoules were sufficient to initiate the gold nano-shell doped K-6 with an 800μm spot size in times scales of ~ 10 milliseconds using extremely short initial pressing column lengths of 3 mm – followed by a wider 5 mm diameter layer of un-doped K-6 that was pressed to a column length of 2 mm. In experimenting with smaller fills of doped K-6 to determine the minimum mass of K-6 needed to achieve detonation, the smallest diameter column that repeatedly detonated was 0.094 inches in diameter pressed at moderate density to a column length of 3-mm for a doped mass of 20 milligrams followed by a 60 milligram second pressing of un-doped K-6. As mentioned previously, a separate pressing die was used to more carefully control the density and uniformity of the initial pressing. A SEM image of the ball-milled HGNs doped K-6 powder is shown in Figure 5 and at the low resolution of the image, the 43 nm diameter HGNs are visible as small bright points on the surface of the crystal as they are too small to be individually imaged at this magnification.

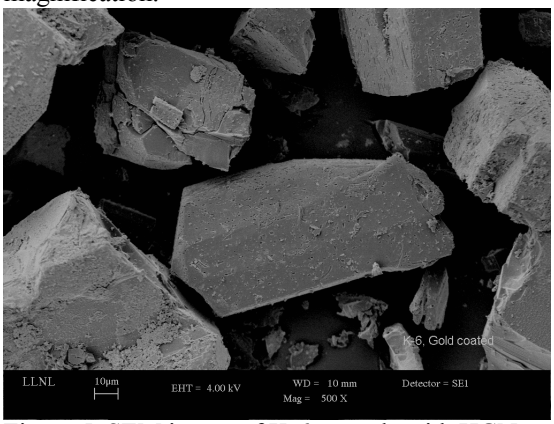

Figure 5. SEM image of K-6 crystals with HGNs

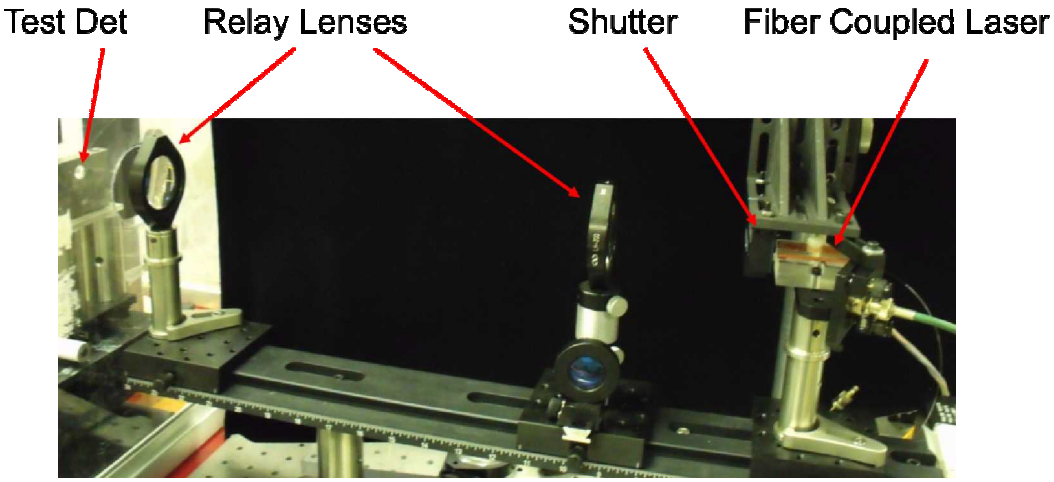

Figure 6. Laser Illumination System to put ~10 watts of 810-nm laser light onto Laser Detonator

Table 1. HMX Laser Det shots with a 1000μ Diameter Spot size

Laser Det	Power (w)	Material	Function t	Energy (mJ)	Spot (mm)
6	11.8	HMX	13.75 ms	162.25	1.00
10	11.8	HMX	8.63 ms	101.83	1.00
11	11.8	HMX	10.58 ms	124.84	1.00
12	11.8	HMX	12.89 ms	152.10	1.00
13	11.8	HMX	12.25 ms	144.55	1.00
14	11.8	HMX	10.80 ms	127.44	1.00

Mean	11.48 ms	137.12
Std Dev	1.69 ms	19.95

Table 2. Keto-RDX (K-6) Laser Det shots with a 1000µ Diameter Spot size

Laser Det	Power (w)	Material	Function t	Energy (mJ)	Spot (mm)
10	10.8	K-6	17.08 ms	184.46	1.00
14	10.8	K-6	24.56 ms	265.25	1.00
16	10.8	K-6	19.03 ms	205.52	1.00
18	10.8	K-6	24.07 ms	259.96	1.00
13	10.8	K-6	24.17 ms	261.04	1.00
		Mean	21.78 ms	235.25	
		Std Dev	3.11 ms	33.58	

Table 3. Keto-RDX (K-6) Laser Det shots with an 800µ Diameter Spot size

Laser Det	Power (w)	Material	Function t	Energy (mJ)	Spot (mm)
28	10.8	K-6	12.87 ms	139.00	0.80
12	10.8	K-6	16.70 ms	180.36	0.80
1	10.8	K-6	15.03 ms	162.32	0.80
2	10.8	K-6	17.13 ms	185.00	0.80
20	10.8	K-6	13.35 ms	144.18	0.80
21	10.8	K-6	15.99 ms	172.69	0.80
22	10.8	K-6	16.03 ms	173.12	0.80
17	10.8	K-6	13.07 ms	141.16	0.80
29	10.8	K-6	14.79 ms	159.73	0.80
25	10.8	K-6	14.87 ms	160.60	0.80
27	10.8	K-6	14.39 ms	155.41	0.80
3	10.8	K-6	14.07 ms	151.96	0.80
7	10.8	K-6	14.52 ms	156.82	0.80
24	10.8	K-6	12.12 ms	130.90	0.80
6	10.8	K-6	15.16 ms	163.73	0.80
8	10.8	K-6	15.37 ms	166.00	0.80
28	10.8	K-6	12.08 ms	130.46	0.80
31	10.8	K-6	12.27 ms	132.52	0.80
		Mean	14.43 ms	155.89	
		Std Dev	1.50 ms	16.23	

Acknowledgements

The author wishes to acknowledge the help and assistance of Constantine Hrousis, Chadd May, Ralph Hodgin, Dan Phillips, Don Hansen, Jim Varosh, and Jon Price in getting the material funding, equipment, and various discussions which fomented this research.

Auspices

This work was performed under the auspices of the U.S. Department of Energy by Lawrence Livermore National Laboratory under contract DE-AC52-07NA27344. Lawrence Livermore National Security, LLC

References

1. Schwartzberg A.M., Olson T.Y., Talley C.E., Zhang J.Z., Synthesis, characterization, and tunable optical properties of hollow gold nanospheres. J Phys Chem B. 2006;**110**:19935–19944.

2. Hafenrichter ES, Pahl RJ, "Characterizing the Effects of Heating Rate and Scale on Microscale Explosive Ignition Criteria" Sandia National Laboratory Report SAND2005-0072, 2005.

3. Gifford M.J., Luebcke P.E., Field J.E., A new mechanism for deflagration-to-detonation in porous granular explosives J. Appl. Phys. **86**, 1749 (1999).

4. Golovina N.I., Goncharov T.K., Dubikhin V.V., Nazin G.M., Shilov G.V., Shu Yu., Kinetics and Mechanism of Thermal Decomposition of Keto-RDX. Russ. J. Phys. Chem. B, 2009, Vol 3, No.6 pp. 896-900.

5. Sikder N, Bulakh NR, Sikder AK, Sarwade DB, Synthesis, characterization and thermal studies of 2-oxo-1,3,5-trinitro-1,3,5-triazacyclohexane (Keto-RDX or K-6) *J. Hazardous Materials*, Vol. **A96**, pp. 109-119, 2003.

6. Mitchell AR, Pagoria PF, Coon CL, Jessop ES, Poco JF, Tarver CM, Breithaupt RD, Moody GL, Synthesis, Scale-up, and Characterization of K-6, Lawrence Livermore Lab Report UCRL-LR-109404, 1991.

7. Glass M.W., Merson J.A., and Salas F.J., "Modeling Low Energy Laser Ignition of Explosive and Pyrotechnic Powders", Proceedings of the Eighteenth International Pyrotechnics Seminar, Breckenridge, CO, 12- 17 July 1992, p. 321.